

RESEARCH ARTICLE

10.1002/2013JD020490

Key Points:

- Atmospheric freezing level heights over High Asia have significantly increased
- Observed rapid deglaciation correlates with changes in freezing level heights
- The climatic significance of freezing level heights is discussed

Correspondence to:

M. Zhang,
mjzhang2004@163.com

Citation:

Wang, S., M. Zhang, N. C. Pepin, Z. Li, M. Sun, X. Huang, and Q. Wang (2014), Recent changes in freezing level heights in High Asia and their impact on glacier changes, *J. Geophys. Res. Atmos.*, 119, 1753–1765, doi:10.1002/2013JD020490.

Received 3 JUL 2013

Accepted 28 JAN 2014

Accepted article online 30 JAN 2014

Published online 25 FEB 2014

Recent changes in freezing level heights in High Asia and their impact on glacier changes

Shengjie Wang¹, Mingjun Zhang^{1,2}, N. C. Pepin³, Zhongqin Li^{1,2}, Meiping Sun¹, Xiaoyan Huang⁴, and Qiong Wang¹

¹College of Geography and Environmental Science, Northwest Normal University, Lanzhou, China, ²State Key Laboratory of Cryospheric Science/Tianshan Glaciological Station, Cold and Arid Regions Environmental and Engineering Research Institute, Chinese Academy of Sciences, Lanzhou, China, ³Department of Geography, University of Portsmouth, Portsmouth, UK, ⁴Institute of Arid Meteorology of China Meteorological Administration, Key Laboratory of Arid Climate Change and Reducing Disaster of Gansu Province, Key Open Laboratory of Arid Climate Change and Reducing Disaster of China Meteorological Administration, Lanzhou, China

Abstract The heights of the atmospheric freezing level have increased over most glacierized areas of High Asia during 1971–2010, especially in the Altai Mountains, the eastern Tianshan Mountains, and the northeastern margins of the Tibetan Plateau. The systematic increase of freezing level heights (FLHs) is evidenced from both radiosonde and National Centers for Environmental Prediction/National Center for Atmospheric Research reanalysis data. Eleven glaciers with long-term observations are selected in typical high-elevation mountain ranges to examine the relationship between changes in FLHs and cryospheric response. Long-term trends in glacier mass balance and equilibrium line altitude (ELA) show significant correlations with changes in FLHs. A rise of 10 m in summer FLH causes mass balance of reference glaciers in High Asia to decrease by between 7 and 38 mm (water equivalent) and ELA to increase by between 3.1 and 9.8 m, respectively, depending on location. Both relationships are statistically significant ($p < 0.01$) for most reference glaciers. Thus, rapid deglaciation in these high mountain ranges during recent decades is related to the increase in FLH. Similar relationships may exist in other high-elevation glaciers of High Asia with changes in FLHs having significant ecological and social consequences, especially in arid and semiarid regions.

1. Introduction

The atmospheric freezing level height (FLH) is a strong control of freeze-thaw processes in high-elevation regions [Diaz and Graham, 1996; Harris *et al.*, 2000; Thurai *et al.*, 2003; Diaz *et al.*, 2003; Bradley *et al.*, 2009; Folkins, 2013]. Changes in the free-air 0°C isotherm affect the high-elevation cryosphere, as ice mass balance is controlled by precipitation type (liquid or solid) and surface albedo [Fujita and Ageta, 2000; Fujita, 2008a, 2008b; Li *et al.*, 2011], both of which are sensitive to temperature. Regions near the annual 0°C isotherm in the extratropics have exhibited among the strongest warming rates in the twentieth century [Pepin and Lundquist, 2008].

In the past decades, most glaciers in High Asia have experienced significant shrinkage in area, length and volume [Fujita and Nuimura, 2011; Wang *et al.*, 2011; Bolch *et al.*, 2012; Yao *et al.*, 2012; Gardner *et al.*, 2013]. Previous research has also indicated that mean FLH in all the major continental mountain chains (including the Himalayas) has exhibited upward shifts during 1948–2000 [Diaz *et al.*, 2003]. In High Asia, summer FLH has showed predominantly upward trends during 1958–2005, being consistent with retreat of the cryosphere [Zhang and Guo, 2011]. In arid regions of Northwest China, there is a strong positive correlation between runoff and FLH, and the proportion of glacial meltwater in runoff is an important driver of this relationship [Zhang *et al.*, 2010; Chen *et al.*, 2012].

Systemic monitoring of the cryosphere (especially using in situ observations) and its relationships with free-air temperature is necessary for understanding the larger-scale climate drivers of current glacier shrinkage. While there are detailed studies in some parts of the world including the tropical Andes [Vuille *et al.*, 2008; Rabatel *et al.*, 2013], East Africa [Mölg *et al.*, 2009] and many extratropical locations [Haeberli *et al.*, 2007; Li *et al.*, 2011], studies of the impact of FLH changes on cryospheric change based on long-term glaciological and hydrometeorological observations are still limited, especially in High Asia. In this paper, we focus on FLH changes near eleven glaciers across the region to examine the broad context of cryospheric change over High Asia for the past several decades.

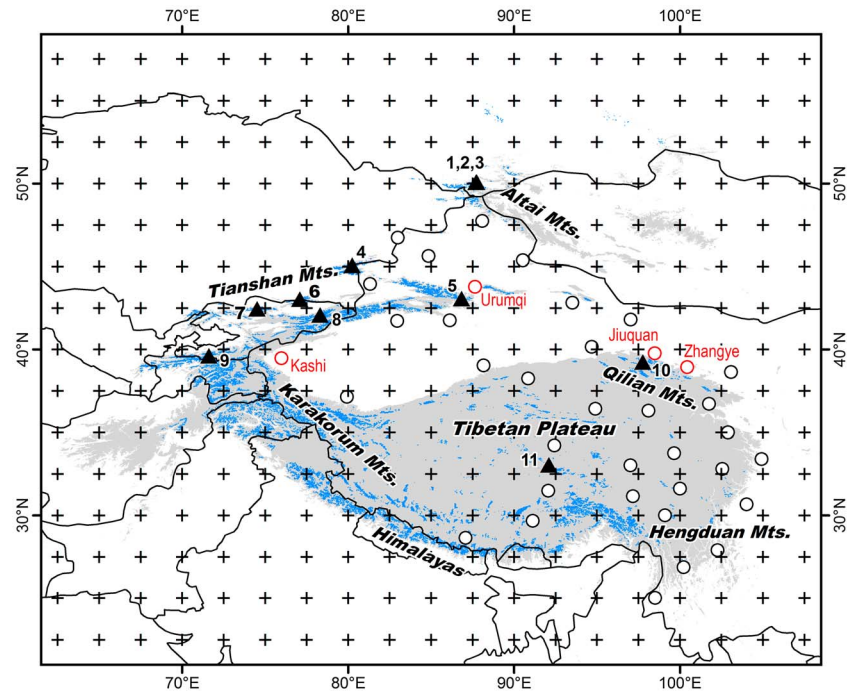


Figure 1. Map showing the distribution of grid boxes (crossed) in NCEP/NCAR reanalysis and radiosonde stations (open circles) in the observation network of the China Meteorological Administration. Four stations shown in Figure 6 are depicted by red circles. Grey and blue shadings indicate elevation higher than 2500 m asl, and glaciers [WGMS and NSIDC, 1989, updated 2012]. Selected glaciers are marked as black triangles. Details are listed in Table 1.

2. Data and Methods

The National Centers for Environmental Prediction (NCEP)/National Center for Atmospheric Research (NCAR) reanalysis R1 from 1971 to 2010 was used to describe the spatial distribution of FLH in High Asia [Kistler *et al.*, 2001]. Mean monthly temperatures at seven mandatory pressure levels (1000, 925, 850, 700, 600, 500, and 400 hPa) were examined to determine the transition from negative temperature ($<0^{\circ}\text{C}$) to ice point or positive temperature ($\geq 0^{\circ}\text{C}$). To cover the area of modern glaciers in High Asia, grid boxes within the ranges of 20–60°N and 60–110°E were used (Figure 1). Monthly FLH were obtained for each grid box via linear interpolation between corresponding geopotential heights [Bradley *et al.*, 2009; Harris *et al.*, 2000]. Monthly FLH for each grid box were combined to calculate summer FLH (arithmetic mean in June, July, and August). Due to the absence of inversions during summer, FLH could be easily defined and there are no negative geopotential heights or multiple heights.

To examine the reliability of FLH derived from NCEP/NCAR reanalysis, we also calculated FLH using the radiosonde data set operated by the China Meteorological Administration (Figure 1). Monthly upper air data at four mandatory pressure levels (850, 700, 500, and 400 hPa) for 37 stations during 1971–2010 was acquired from the National Meteorological Information Center (NMIC) of the China Meteorological Administration. The radiosonde ascents were observed at 00 and 12 UTC (08 and 20 Beijing Time).

Homogeneity testing is particularly important when assessing trends. Therefore a series of quality control checks were employed by *National Meteorological Information Center* [2005], including checks for high-low extreme values, internal consistency, temporal consistency, and hydrostatic tests. Homogeneity was assessed through the penalized maximal F test (PMFT) [Wang, 2008; Xu *et al.*, 2013]. At each mandatory pressure level, the two time series at 00 and 12 UTC were averaged on a monthly basis to test for homogeneity. Possible change points in monthly geopotential height and temperatures were identified and adjusted when there was supporting metadata (e.g., instrument updates, algorithm changes, etc.). The homogenized series were used in calculation of the monthly FLH. At each radiosonde station FLH was calculated via linear interpolation between the relevant geopotential heights, and again summer FLH was the arithmetic mean of FLH in June, July, and August (similar to reanalysis data). No correction was made for the different number of days in the 3 months.

Table 1. Inventory of Selected Glaciers Over High Asia^a

No.	Glacier Name	Mountain Range	Country	Latitude (°N)	Longitude (°E)	Period	Data Source
1	No.125 (Vodopadny)	Altai	Russia	50.10	87.70	1977–2009	Dyurgerov [2002]; WGMS [2005, 2008, 2012]
2	Leviy Aktru	Altai	Russia	50.08	87.72	1977–2009	Dyurgerov [2002]; WGMS [2005, 2008, 2012]
3	Maliy Aktru	Altai	Russia	50.08	87.75	1971–2009	Dyurgerov [2002]; WGMS [2005, 2008, 2012]
4	Shumskiy	Dzhungarskiy	Kazakhstan	45.08	80.23	1971–1991	Dyurgerov [2002]
5	Urumqi No.1	Tianshan	China	43.08	86.82	1971–2010	Ye et al. [2005]; WGMS [2008, 2012]
6	Ts. Tuyuksuyskiy	Tianshan	Kazakhstan	43.05	77.08	1971–2010	Dyurgerov [2002]; WGMS [2005, 2008, 2012]
7	Golubin	Tianshan	Kyrgyzstan	42.47	74.50	1971–1994	Dyurgerov [2002]
8	Kara-Batkak	Tianshan	Kyrgyzstan	42.10	78.30	1971–1998	Dyurgerov [2002]; WGMS [2005]
9	Abramov	Pamir	Kyrgyzstan	39.63	71.60	1971–1998	Dyurgerov [2002]
10	Qiyi	Qilian	China	39.25	97.75	1974–2010	Wang et al. [2010]; Yao et al. [2012]
11	Xiao Dongkemadi	Tanggula	China	33.07	92.08	1989–2010	Fujita et al. [2000]; Pu et al. [2008]; Yao et al. [2012]; Zhang et al. [2013]

^aLocations are depicted in Figure 1; WGMS = World Glacier Monitoring Service.

For most glaciers in High Asia, maximum accumulation and ablation occur simultaneously during the warm wet summer, because summer precipitation makes up a large proportion of the annual amount. This is different from the European Alps which are nourished by winter precipitation in the westerlies [Shi, 2008]. Summer is the critical season in determining glacier mass balance in High Asia, so we focus on the relationship between glacier parameters and mean summer FLH. A total of 11 glaciers with long-term records (≥ 15 years) of mass balance and equilibrium line altitude (ELA) were chosen (Figure 1 and Table 1). Mass balance and ELA were calculated from field measurements, usually made at the end of each ablation season, i.e., late September/early October [Yao et al., 2012]. For glacier parameters, the year 1971 covers the water year October 1970 to September 1971.

The selected glaciers are mainly located in the Tianshan and Altai Mountains. On the Tibetan Plateau (including the marginal ranges such as Karakorum, Qilian, Himalayas, Hengduan), fieldwork has been widely implemented in recent decades [Kang et al., 2010; Yao et al., 2012; M \ddot{o} lg et al., 2014] but continuous records of

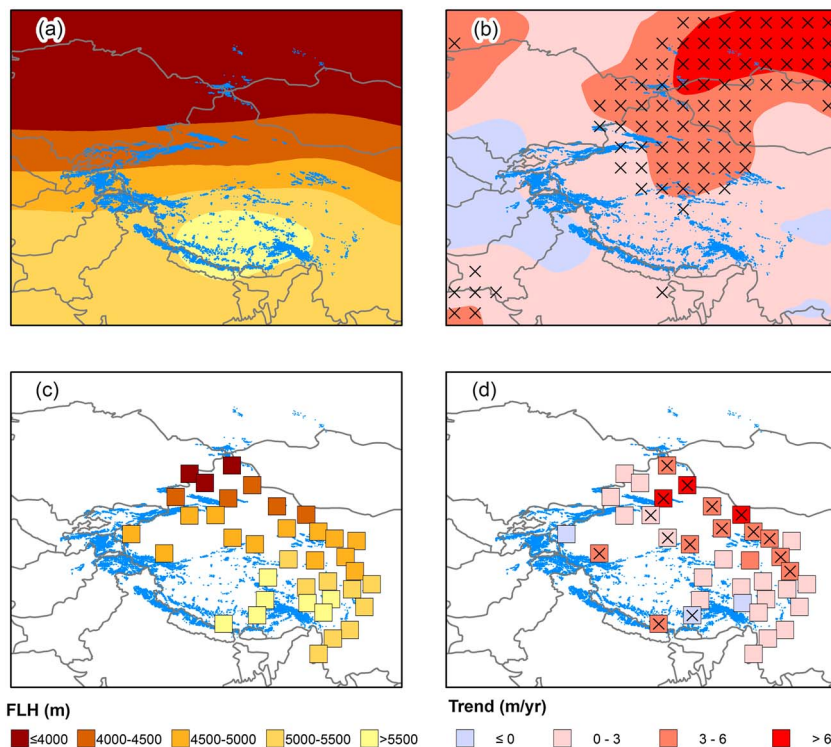


Figure 2. Arithmetic mean of summer (JJA) freezing level height (FLH) and linear trends in summer FLH for the years 1971–2010 based on (a and b) NCEP/NCAR reanalysis data and (c and d) radiosonde data of the China Meteorological Administration. Grid boxes with trends significant at $p < 0.05$ are indicated with crosses. Glaciers are shaded in blue according to the World Glacier Inventory [WGMS and NSIDC, 1989, updated 2012].

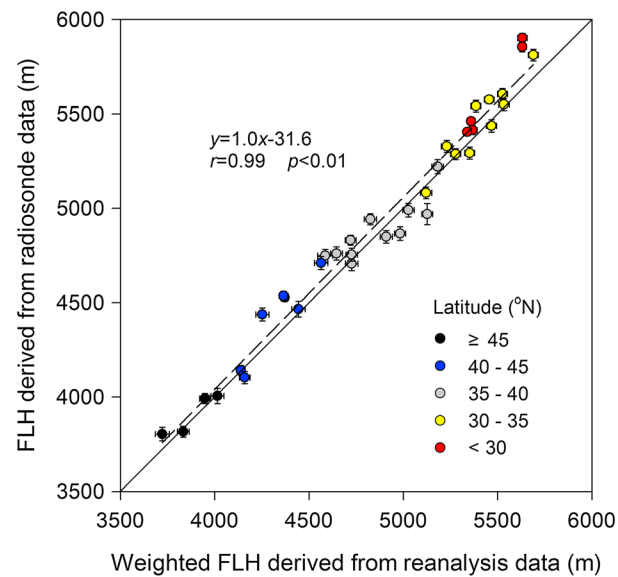


Figure 3. Correlation between mean summer (JJA) freezing level heights (FLHs) at radiosonde stations and summer FLH interpolated from NCEP/NCAR reanalysis data (1971–2010). The line of equality is shown as a solid line. Error bars denote 95% confidence interval.

mass balance and ELA are generally less than two decades in length, so our analysis on the plateau is limited to two sites (sites 10 and 11).

Two other surface data sets were also employed. (a) To examine the relationship between radiosonde-based FLH (usually observed over low-lying areas) and surface air temperature at equivalent elevations relevant to glacial systems, monthly surface air temperatures taken from a subset of national meteorological stations in China for the period 1971–2010 were used (for the spatial distribution of candidate stations, see *Xu et al.* [2013]). The data are provided by the NMIC and the Xinjiang Meteorological Bureau. Homogeneity tests and necessary adjustments had been carried out through a penalized maximal F test (PMFT) [*Wang*, 2008]. Details of station selection are discussed later. (b) the Global Precipitation Climatology Centre Full Data Reanalysis Product Version 6 [*Schneider et al.*, 2011], a data set of gridded monthly precipitation with spatial resolution of $0.5^\circ \times 0.5^\circ$, was used to analyze the spatial distribution of summer precipitation over 1971–2010. Data processing and accuracy assessment are described in *Schneider et al.* [2014] and *Becker et al.* [2013].

In order to compare radiosonde and reanalysis based FLH (1971–2010), the reanalysis data was interpolated to the same positions as the radiosonde stations, through inverse distance weighting of the nearest four grid boxes. Sen's nonparametric method [*Sen*, 1968] was used to calculate linear trends in FLH. The trend-free prewhitening procedure [*Yue et al.*, 2002; *Yue and Wang*, 2002] was applied to detect significance, taking into account serial autocorrelation. A trend is statistically significant if it is significant at $p < 0.05$. For the calculation of correlation coefficients, Pearson's correlation coefficient and two-tailed t tests were applied.

3. Results

3.1. FLH Changes in High Asia

Arithmetic means of summer (JJA) FLH in High Asia are shown in Figures 2a (NCEP/NCAR reanalysis) and 2c (radiosondes). Spatial patterns of FLH derived from the two data sources are similar. Summer FLH generally declines from the tropics to the arctic and thus summer FLH ranges from >5500 m in the Himalayas to ~ 3000 m in the Altai Mountains. Relatively high summer FLH are found over the middle and southern Tibetan Plateau around $80\text{--}100^\circ\text{N}$ and $25\text{--}35^\circ\text{E}$.

Figures 2b (NCEP/NCAR) and 2d (radiosondes) demonstrate linear trends of summer FLH during 1971–2010. According to NCEP/NCAR reanalysis, most heights (86.6% of the grid boxes within $60\text{--}110^\circ\text{E}$ and $20\text{--}60^\circ\text{N}$) have increased, especially in the north of High Asia. 29.4% of the grid boxes in the region have trends significant at the 0.05 level, mainly in the Altai Mountains, the eastern Tianshan Mountains, and the northern margin of the Tibetan

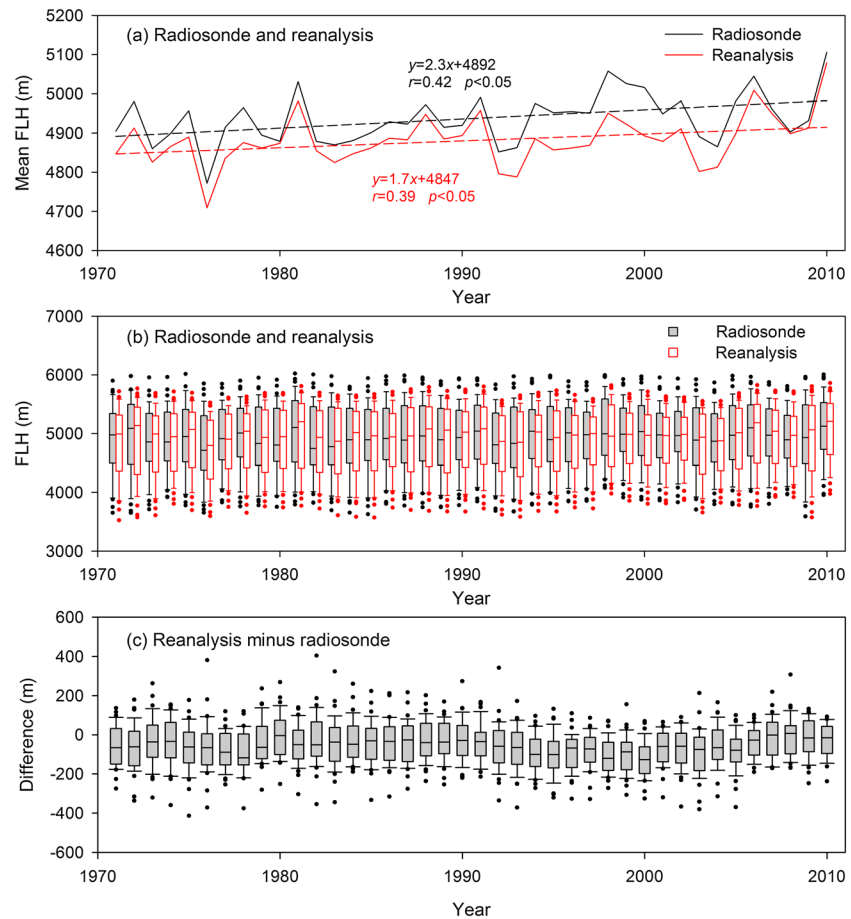


Figure 4. (a) Temporal variation of regionwide arithmetic mean of summer (JJA) freezing level height (FLH) at all radiosonde stations and arithmetic mean of weighted summer FLH derived from NCEP/NCAR reanalysis data (all grid boxes) for 1971–2010. (b) Annual box plots of mean summer (JJA) FLH at radiosonde stations and reanalysis grid boxes for 1971–2010. The lower boundary of the box indicates the 25th percentile, a line within the box marks the fiftieth percentile (median), and the upper boundary of the box indicate the 75th percentile; whiskers (error bars) above and below the box indicate the ninetieth and tenth percentiles; points above and below the whiskers indicate outliers. (c) Annual box plots of the difference between mean summer (JJA) FLH at radiosonde stations and at reanalysis grid points for 1971–2010.

Plateau. At the western margin of Tibetan Plateau (Figure 2c), FLH have decreased slightly, but these changes are not statistically significant. FLH derived from radiosondes shows generally similar spatial patterns (Figure 2d), and the average trend is 27 m per decade (individual trends range from –25 to 80 m per decade). FLH at 91.9% of the radiosonde stations have increased, and 40.5% of stations show a statistically significant increase ($p < 0.05$). Thus overall changes appear to be more widespread in the radiosonde data than in the reanalysis.

We compared FLH obtained from the observational radiosonde series to that derived from NCEP/NCAR reanalysis at each station using inverse distance weighting (Figure 3). Mean summer FLH for each station derived from the two data sets correlate well ($r=0.99$, $p < 0.01$, $n = 37$). Generally, FLH derived from radiosonde stations are higher than those from reanalysis, especially between 40°N and 45°N. Thus, the slope of linear fit is slightly above the diagonal line of equality. The gradient of the regression line is slightly less than 1, meaning that the intercept is slightly below sea level.

Figure 4a shows the variation of regionwide FLHs (arithmetic average FLH derived from all radiosonde stations or equivalent interpolated reanalysis locations) for the two contrasting data sources during the past four decades. The trend magnitude of the radiosonde-based series is approximate 2.3 m/yr, with that of the reanalysis-based series slightly lower (1.7 m/yr). Both trends are statistically significant ($p < 0.05$). Annual box plots for the two series are displayed in Figure 4b. Although the arithmetic average FLH for each year derived from radiosonde stations is always higher than that from NCEP/NCAR reanalysis, the median FLH

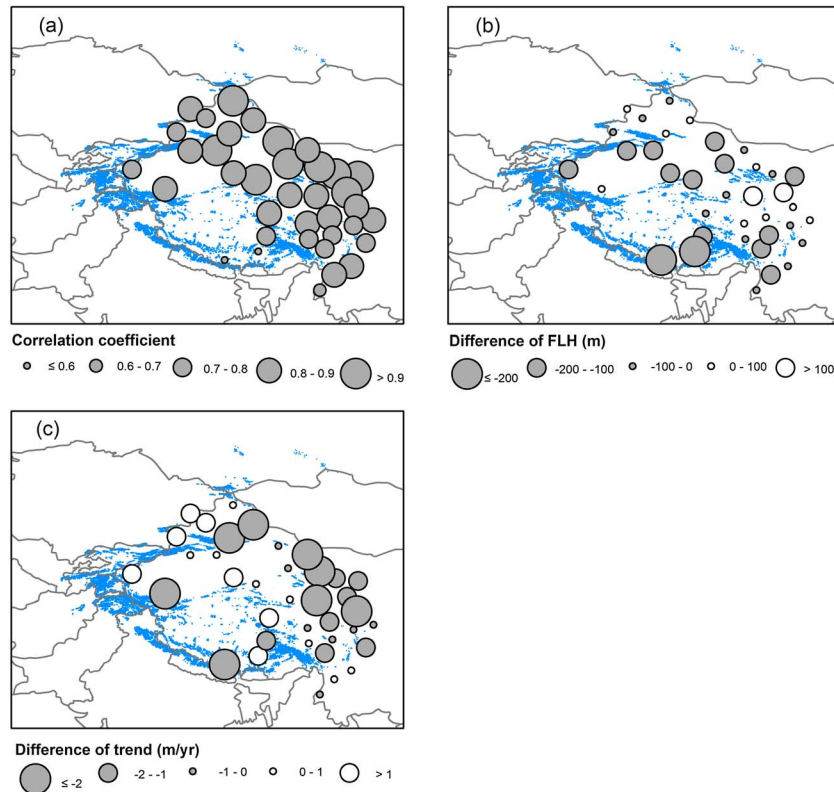


Figure 5. (a) Spatial distribution of anomaly correlations between summer (JJA) freezing level heights (FLH) derived from radiosonde stations and interpolated reanalysis data (1971–2010). Glaciers are shaded in blue according to the World Glacier Inventory [WGMS and NSIDC, 1989, updated 2012]. (b) Spatial distribution of the mean difference between mean summer (JJA) FLH at radiosonde stations and equivalent interpolated reanalysis location (1971–2010) (reanalysis minus radiosonde). (c) Spatial distribution of the difference in linear trend magnitude between summer (JJA) FLH at radiosonde stations and equivalent interpolated reanalysis location (1971–2010) (reanalysis minus radiosonde).

values for the two series exhibit less systematic differences. All outliers (top and bottom 10%) are marked in Figure 4b. Extreme high FLHs derived from radiosonde stations are generally higher than in the reanalysis. However, no significant increase or decrease can be found in the difference between the two FLHs (Figure 4c).

A good test of the compatibility of the two data sets is to examine the spatial distribution of the correlation between summer FLH anomalies derived from the two methods (radiosonde versus reanalysis) (Figure 5a). Higher values are located in the northeastern parts of High Asia and correlations weaken a little over the more topographically complex southern regions (sometimes less than 0.6). Regions with high correlations also generally show significant FLH increase. Figure 5b shows the difference in mean FLH between the two data sets (reanalysis minus radiosonde). Negative values found at most stations mean that the reanalysis FLH is lower (colder temperatures), but there are exceptions over the eastern part of the Tibetan Plateau. The spatial pattern of the difference (reanalysis minus radiosonde) between the two FLH trends (shown separately in Figures 2b and 2d) is shown in Figure 5c. In the western and middle parts of High Asia reanalysis trends are more positive (more rapid warming), but the opposite is the case in eastern parts of the region. Although the overall pattern is variable, there is some regional coherence to the trend contrasts.

3.2. Relationship Between FLH and Surface Temperature

To compare free-air FLH (recorded above radiosonde stations) and surface temperatures at equivalent elevations in the vicinity of glaciers, monthly surface air temperatures (2 m screen level) at national meteorological stations in China surrounding each radiosonde station were selected for comparison. However, to make a reasonable comparison only four regions were chosen according to the following criteria: (1) the specific radiosonde station had at least three surface stations within 150 km; (2) the altitudinal range of these ground stations was at least 2000 m; and (3) glaciers were within 100 km of the highest surface station. The four regions surround radiosonde

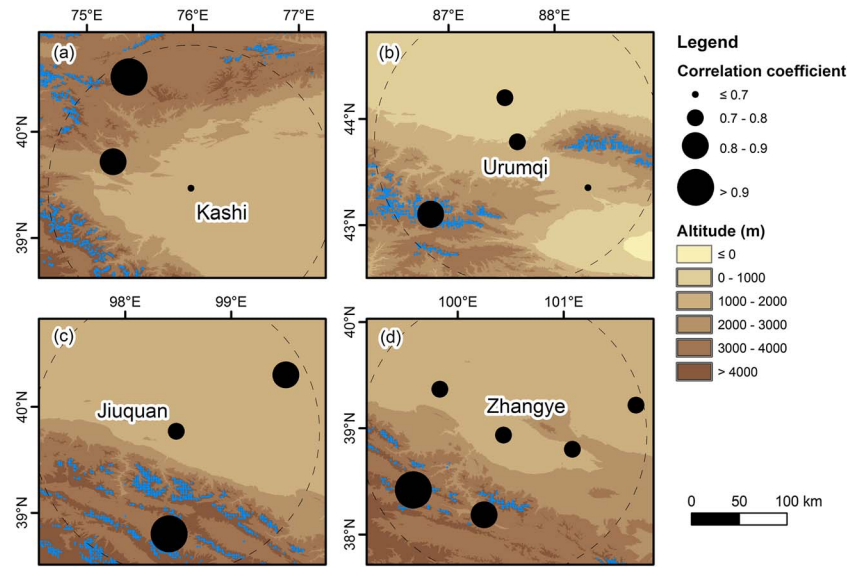


Figure 6. Spatial distribution of correlation coefficient between summer (JJA) freezing level height (FLH) recorded above specific radiosonde stations and summer surface air temperatures at neighboring ground meteorological stations in four selected regions in High Asia for the years 1971–2010. The radiosonde stations are (a) Kashi, (b) Urumqi, (c) Jiuquan, and (d) Zhangye, respectively. Glaciers are shaded in blue according to the World Glacier Inventory [WGMS and NSIDC, 1989, updated 2012]. The dashed circles denote the horizontal distance of 150 km from the central radiosonde station.

stations at Kashi, Urumqi, Jiuquan, and Zhangye (Figure 6). Kashi and Urumqi lie on the southern and northern slopes of the Tianshan Mountains, respectively. Jiuquan and Zhangye are located on the northern slopes of the Qilian Mountains (northeastern margin of the Tibetan Plateau).

As is shown in Figure 6, for each selected region, the correlation coefficients between summer (JJA) FLH and surface temperatures at alpine stations (higher altitude) are generally higher than at lower stations. Often the correlation with surface temperature at the radiosonde station itself is lower than with higher stations further afield (e.g., Urumqi) (Figures 6b and 7). Figure 7 demonstrates the relationship between radiosonde-derived FLH above Urumqi (935 m above sea level (asl)) and air temperature measured at surrounding stations.

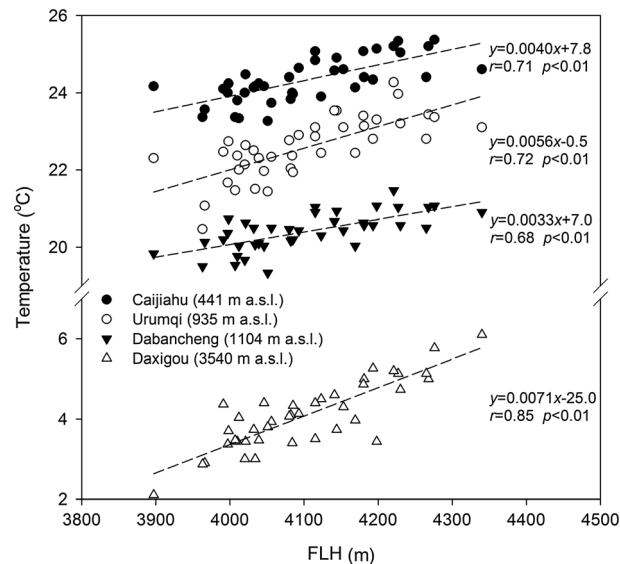


Figure 7. Relationship between summer (JJA) freezing level height (FLH) at radiosonde station Urumqi and summer surface air temperature at neighboring ground meteorological stations (Caijiahu, Urumqi, Dabancheng, and Daxigou) for 1971–2010.

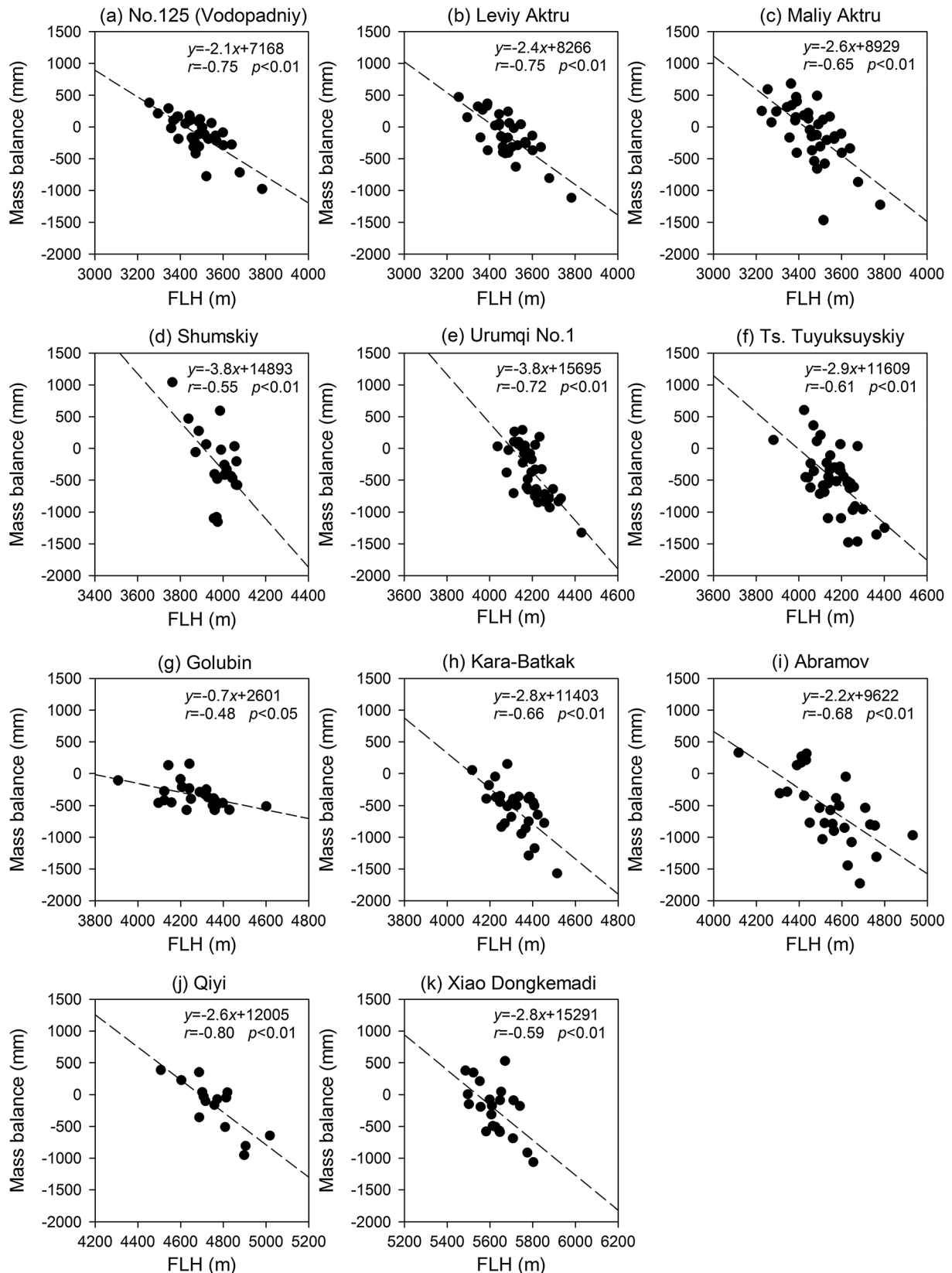


Figure 8. Correlation between annual mass balance for selected glaciers and summer (JJA) freezing level height (FLH) derived from NCEP/NCAR reanalysis data for 1971–2010. FLH are interpolated from the nearest four grid points.

Table 2. Linear Regressions Between Glacial Parameters (Mass Balance and Equilibrium Line Altitude) of Selected Glaciers in High Asia and Weighted Summer (JJA) Freezing Level Height (FLH) Derived From NCEP/NCAR Reanalysis (1971–2010)

No.	Glacier Name	Mass Balance versus FLH			Equilibrium Line Altitude versus FLH		
		Slope (mm/m)	r^a	n^a	Slope (m/m)	r	n
1	No.125 (Vodopadnyi)	-2.1*	-0.75	33	0.52*	0.62	30
2	Leviy Aktru	-2.4*	-0.75	33	0.57*	0.70	33
3	Maliy Aktru	-2.6*	-0.65	39	0.68*	0.62	39
4	Shumskiy	-3.8*	-0.55	21	0.42*	0.58	19
5	Urumqi No.1	-3.8*	-0.72	40	0.77*	0.65	40
6	Ts. Tuyuksuyskiy	-2.9*	-0.61	40	0.64*	0.53	40
7	Golubin	-0.7**	-0.48	24	0.34*	0.58	23
8	Kara-Batkak	-2.8*	-0.66	28	0.31	0.34	23
9	Abramov	-2.2*	-0.68	28	0.49*	0.71	27
10	Qiyi	-2.6*	-0.80	15	0.98**	0.59	16
11	Xiao Dongkemadi	-2.8*	-0.59	22	0.71	0.48	16

^aThe correlation coefficient of linear regression is r , and n is the number of years of available data.

*Statistically significant at the 0.01 level.

**Statistically significant at the 0.05 level.

The strongest similarity is shown at Daxigou (3540 m asl) with cold summers being reflected in lower than normal FLH, and vice versa. For the low-lying desert station Caijiahu (441 m asl), the correlation between FLH and surface air temperature is much lower ($r=0.71$) than that at the alpine station Daxigou ($r=0.85$). This is because of frequent low-level temperature inversions and thus more frequent decoupling of surface climate from the free air at lower elevations, and implies more consistent regional temperatures at higher elevations.

3.3. Influence of FLH Change on Glacier Fluctuation

Glacier mass balance and equilibrium line altitude (ELA) are used to investigate the impact of FLH changes on glacier fluctuation. Because of the good spatial continuity of NCEP/NCAR reanalysis derived FLH over the glacier-covered areas in High Asia, and the fact that radiosonde stations in China are generally far away from the glaciers selected, reanalysis data are used to calculate FLH at reference glacier locations. Figure 8 shows the correlations between mass balance and summer FLH (interpolated using inverse distance weighting from the four nearest reanalysis grid points) for each adjacent reference glacier. Although correlations are not perfect, there are negative correlations in all cases and r values are below -0.5 except for the Golubin Glacier in the western Tianshan Mountains. For Qiyi Glacier in the Qilian Mountains, $r=-0.80$. Detailed regression coefficients for each glacier are shown in Table 2. A rise of 10 m in FLH can cause mass balance to decrease by between 21 and 38 mm w.e. depending on the glacier (with an exception of 7 mm w.e. for Golubin Glacier). Most relationships are statistically significant at $p < 0.01$.

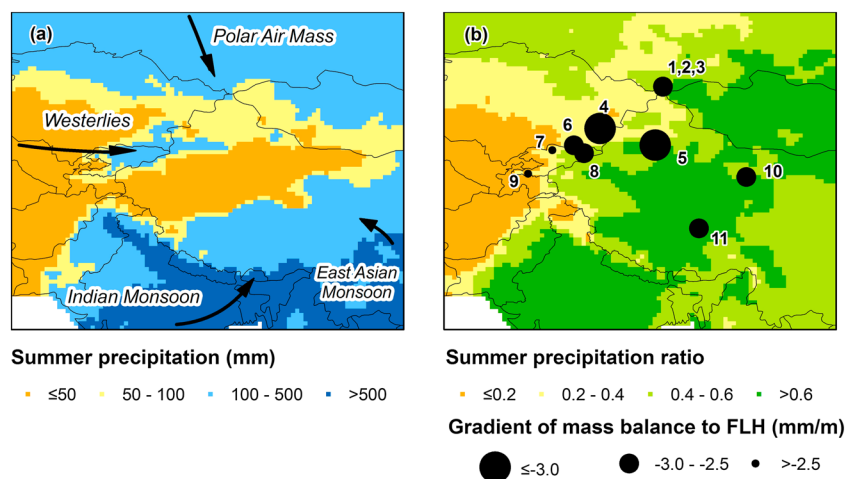


Figure 9. Spatial distribution of arithmetic mean of (a) summer (JJA) precipitation for the years 1971–2010 and (b) ratio of summer (JJA) to annual precipitation, derived from the Global Precipitation Climatology Centre Full Data Reanalysis Product Version 6 [Schneider et al., 2011]. The gradients of mass balance of selected glaciers to FLH are also shown in Figure 9b.

Generally, high values of FLH coincide with negative values of mass balance and vice versa. Using No.125 (Vodopadni) Glacier (Figure 8a) in the Russian Altai Mountains as an example, the observed lowest mass balance (-980 mm w.e.) occurs in 1998. Coincidentally, summer FLH in 1998 was 3784 m, 316 m higher than the mean height (3468 m) during the study period. Similar correspondences also exist in other years. For the other 10 glaciers, the fluctuations of mass balance and summer FLH generally show an inverse relationship.

Relationships with ELA are also shown in Table 2. Summer FLH shows positive correlations with ELA (mostly significant at $p < 0.01$), but the correlation coefficients are generally lower than those for mass balance. A rise of 10 m in FLH can cause ELA to increase by between 3.1 and 9.8 m depending on the glacier.

Despite significant relationships between FLH and temperature, precipitation is also important in glacier accumulation and melt, so this in part explains the different gradients of glacier mass balance to FLH in Table 2. Figures 9a and 9b thus shows the spatial distribution of mean summer precipitation amount and the ratio of summer precipitation (JJA) to annual precipitation between 1971 and 2010. Generally, areas with low summer precipitation ratios have weak gradients of glacier mass balance to FLH. This is the case in areas where winter precipitation (controlled by the midlatitude westerly circulation) is dominant such as the Abramov and Golubin glaciers [Mölg *et al.*, 2014].

4. Discussion

The biases within reanalysis data sets including NCEP/NCAR reanalysis have attracted much attention [Simmons *et al.*, 2004; Liu *et al.*, 2012]. In the Tibetan Plateau, surface air temperatures derived from NCEP/NCAR are generally lower than in situ observations, and the reanalysis is considered to be more representative of free-air temperature conditions instead of surface air temperature [You *et al.*, 2013; Bao and Zhang, 2013]. As is shown in Figures 3 and 4, FLH in High Asia derived from NCEP/NCAR reanalysis also tend to be lower than FLH derived from radiosondes. The cold bias present in NCEP/NCAR reanalysis is therefore consistent with its comparison with surface air temperatures [You *et al.*, 2013].

However, this bias does not influence long-term warming trends systematically during the past four decades derived from both data sets as the varied comparison in Figure 5c shows. Furthermore, reanalysis-based FLH have good correlation with that derived from radiosonde stations for most regions in High Asia (Figures 3 and 5a), and thus, the reanalysis can be used for FLH calculation, especially on large-scales.

Previous studies based on high-elevation sites across the globe [Pepin and Seidel, 2005] demonstrated that correlations between monthly surface and free-air temperature anomalies depend on topography but are often high. The correlation between FLH and surface air temperature was shown to vary according to landform and elevation, with exposed summits showing much higher correlations. We find that free-air freezing level heights in High Asia often correlate well with surface temperatures at high elevations near glaciers (often much better than with nearer lowland stations). Thus, as shown in Figures 6 and 7, free-air FLH can reflect the high-altitude surface temperature quite well, and we can estimate surface air temperature from free-air FLH measured some distance away.

Long-term meteorological records near high-altitude glaciers remain important, especially for glacier modeling and other cryospheric research. Despite an extensive glaciated area in western China, in situ observations near glaciers are limited due to remoteness and lack of population. Thus, using FLH to estimate meteorological conditions will still be required. A good example, shown in Figures 6b and 7, is the successful reconstruction of summer temperature at Urumqi Glacier No.1 (Daxigou station) from FLH above Urumqi.

Previous work [Kang *et al.*, 2010; Yao *et al.*, 2012; Zhang *et al.*, 2012] found that the glaciers in the Altai, eastern Tianshan, and Qilian Mountains had experienced particularly rapid retreat during the second half of the twentieth century, and Figure 2 confirms strong increasing trends in FLH in these areas. Climate regimes on glaciers worldwide have been discussed in detail by Ohmura *et al.* [1992], among others. With the increase of summer FLH, surface air temperatures have more frequently risen above freezing, especially at lower altitudes, and this leads to large ice mass loss. Thus, melting is a direct reason for strong correlations between FLH and glacial parameters (mass balance and ELA) shown in Figure 8. However, besides the direct thermal effect, the influence of FLH on spectral albedo should not be ignored. Snow cover is a vital factor influencing surface albedo and net radiation balance. In glacial terms fresh snow cover will increase surface albedo and contribute to enhanced mass balance, both through direct accumulation and through reduction of ablation

[Fujita and Ageta, 2000; Fujita, 2008a, 2008b]. Warming rates at high altitudes are thought to be significantly enhanced by snow-ice feedback across the globe [Pepin and Lundquist, 2008]. Reduced surface albedo in high-altitude mountain ranges (where fresh snowfall is replaced by liquid precipitation, and glacier surfaces become “dirty”) may therefore also be responsible for the accelerated recession of the cryosphere. Previous research on Urumqi Glacier No.1 [Li *et al.*, 2011] has demonstrated reduced albedo on the glacier surface (because of enlarged ablation area, coarsened firn structure, and increased cryoconite granules) and is considered to be an additional mechanism underlying recent recession. It is difficult to estimate actual precipitation near glaciers due to the absence of in situ observations, but the main patterns and trends can be acquired from high-resolution gridded precipitation data sets. Using the gradient of the regression line between mass balance and FLH, we show that sensitivity of mass balance to FLH is usually weaker for glaciers with lower summer precipitation ratios (Figure 9), and in areas such as the western Tianshan Mountains dominated by the westerly circulation.

5. Concluding Remarks

In this paper, we have selected several glaciers with long-term observations in typical high-elevation mountain ranges to examine the spatial variation in the relationship between changes in FLH and cryospheric indicators. According to long-term meteorological and glacial records near the 11 selected reference glaciers, the increase of summer FLH is significantly correlated with the deglaciation process.

FLH are shown to be increasing significantly in High Asia over the last 40 years (1971–2010), both from radiosonde and NCEP/NCAR reanalysis data. This increase may cause significant cryospheric shrinkage, and the changes can be observed as an increase in equilibrium line altitude (ELA) and decreased mass balance. FLH measured above low-lying areas provide an effective method to estimate surface air temperature in many high-altitude mountain ranges, and this method of estimation is required especially in areas without sufficient in situ meteorological observation.

We present a detailed examination of several reference glaciers based on combining field observations with interpolated meteorological records at a range of spatial scales, but almost all the glacier-covered areas in High Asia have experienced an increase of summer FLH in recent decades (based on radiosonde and reanalysis data sets). This spatial pattern has resulted in widespread shrinkage of glaciers not only in the selected reference glaciers but also over almost all of High Asia including the Tibetan Plateau and the surrounding mountain ranges. Rapid glacial retreat during recent decades, including in the Altai, eastern Tianshan, and Qilian Mountains, is mainly concentrated in regions with significantly increasing trends in FLH.

Glacier-fed runoff is an important water resource at middle and lower elevations, and thus, glacier retreat may have significant ecological and social consequences outside the immediate high mountains, especially in interior arid and semiarid regions [Vergara *et al.*, 2007; Piao *et al.*, 2010]. In previous reports [Liu and Chen, 2000; Liu *et al.*, 2009; Qin *et al.*, 2009], analysis of abundant meteorological records during the past decades have showed that high-elevation mountains in High Asia are a sensitive indicator of the global warming signal. Our evidence in this paper showing increased free-air freezing level heights in High Asia and associated rapid retreat of glaciers at high elevations provides further support for this view.

Acknowledgments

This study was supported by the National Basic Research Program of China (973 Program) (2013CBA01801) and the National Natural Science Foundation of China (41161012). We are very grateful to Koji Fujita (Nagoya University) and two anonymous reviewers for their constructive suggestions. Thanks also to the editorial staff.

References

- Bao, X., and F. Zhang (2013), Evaluation of NCEP-CFSR, NCEP-NCAR, ERA-Interim, and ERA-40 Reanalysis datasets against independent sounding observations over the Tibetan Plateau, *J. Clim.*, *26*, 206–214, doi:10.1175/JCLI-D-12-00056.1.
- Becker, A., P. Finger, A. Meyer-Christoffer, B. Rudolf, K. Schamm, U. Schneider, and M. Ziese (2013), A description of the global land-surface precipitation data products of the Global Precipitation Climatology Centre with sample applications including centennial (trend) analysis from 1901-present, *Earth Syst. Sci. Data*, *5*, 71–99, doi:10.5194/essd-5-71-2013.
- Bolch, T., et al. (2012), The state and fate of Himalayan Glaciers, *Science*, *336*, 310–314, doi:10.1126/science.1215828.
- Bradley, R. S., F. T. Keimig, H. F. Diaz, and D. R. Hardy (2009), Recent changes in freezing level heights in the Tropics with implications for the deglaciation of high mountain regions, *Geophys. Res. Lett.*, *36*, L17701, doi:10.1029/2009GL037712.
- Chen, Z., Y. Chen, and W. Li (2012), Response of runoff to change of atmospheric 0°C level height in summer in arid region of Northwest China, *Sci. China Earth Sci.*, *55*, 1533–1544, doi:10.1007/s11430-012-4472-6.
- Diaz, H. F., and N. E. Graham (1996), Recent changes in tropical freezing heights and the role of sea surface temperature, *Nature*, *383*, 152–155, doi:10.1038/383152a0.
- Diaz, H. F., J. K. Eischeid, C. Duncan, and R. S. Bradley (2003), Variability of freezing levels, melting season indicators, and snow cover for selected high-elevation and continental regions in the last 50 years, *Clim. Change*, *59*, 33–52, doi:10.1023/A:1024460010140.
- Dyurgerov, M. (2002), *Glacier Mass Balance and Regime: Data of Measurements and Analysis*, Institute of Arctic and Alpine Research, University of Colorado, Boulder, USA.

- Folkens, I. (2013), The melting level stability anomaly in the tropics, *Atmos. Chem. Phys.*, *13*, 1167–1176, doi:10.5194/acp-13-1167-2013.
- Fujita, K. (2008a), Effect of precipitation seasonality on climatic sensitivity of glacier mass balance, *Earth Planet. Sci. Lett.*, *276*, 14–19, doi:10.1016/j.epsl.2008.08.028.
- Fujita, K. (2008b), Influence of precipitation seasonality on glacier mass balance and its sensitivity to climate change, *Ann. Glaciol.*, *48*, 88–92, doi:10.3189/172756408784700824.
- Fujita, K., and Y. Ageta (2000), Effect of summer accumulation on glacier mass balance on the Tibetan Plateau revealed by mass-balance model, *J. Glaciol.*, *46*, 244–252, doi:10.3189/172756500781832945.
- Fujita, K., and T. Nuimura (2011), Spatially heterogeneous wastage of Himalayan glaciers, *Proc. Natl. Acad. Sci. U. S. A.*, *108*, 14,011–14,014, doi:10.1073/pnas.1106242108.
- Fujita, K., Y. Ageta, J. Pu, and T. Yao (2000), Mass balance of Xiao Dongkemadi glacier on the central Tibetan Plateau from 1989 to 1995, *Ann. Glaciol.*, *31*, 159–163, doi:10.3189/172756400781820075.
- Gardner, A. S., et al. (2013), A reconciled estimate of glacier contributions to sea level rise: 2003 to 2009, *Science*, *340*, 852–857, doi:10.1126/science.1234532.
- Haeberli, W., M. Hoelzle, F. Paul, and M. Zemp (2007), Integrated monitoring of mountain glaciers as key indicators of global climate change: The European Alps, *Ann. Glaciol.*, *46*, 150–160, doi:10.3189/172756407782871512.
- Harris, G. N., Jr., K. P. Bowman, and D.-B. Shin (2000), Comparison of freezing-level altitudes from NCEP Reanalysis with TRMM precipitation radar brightband data, *J. Clim.*, *13*, 4137–4148, doi:10.1175/1520-0442(2000)013<4137:COFLAF>2.0.CO;2.
- Kang, S., Y. Xu, Q. You, W.-A. Flügel, N. Pepin, and T. Yao (2010), Review of climate and cryospheric change in the Tibetan Plateau, *Environ. Res. Lett.*, *5*, 015101, doi:10.1088/1748-9326/5/1/015101.
- Kistler, R., et al. (2001), The NCEP-NCAR 50-year reanalysis: Monthly means CD-ROM and documentation, *Bull. Am. Meteorol. Soc.*, *82*, 247–267, doi:10.1175/1520-0477(2001)082<0247:TNNYRM>2.3.CO;2.
- Li, Z., H. Li, and Y. Chen (2011), Mechanisms and simulation of accelerated shrinkage of continental glaciers: A case study of Urumqi Glacier No. 1 in eastern Tianshan, Central Asia, *J. Earth Sci.*, *22*, 423–430, doi:10.1007/s12583-011-0194-5.
- Liu, X., and B. Chen (2000), Climatic warming in the Tibetan Plateau during recent decades, *Int. J. Climatol.*, *20*, 1729–1742, doi:10.1002/1097-0088(20001130)20:14<1729::AID-JOC556>3.0.CO;2-Y.
- Liu, X., Z. Cheng, L. Yan, and Z.-Y. Yin (2009), Elevation dependency of recent and future minimum surface air temperature trends in the Tibetan Plateau and its surroundings, *Global Planet. Change*, *68*, 164–174, doi:10.1016/j.gloplacha.2009.03.017.
- Liu, Z., Z. Xu, Z. Yao, and H. Huang (2012), Comparison of surface variables from ERA and NCEP reanalysis with station data over eastern China, *Theor. Appl. Climatol.*, *107*, 611–621, doi:10.1007/s00704-011-0501-1.
- Mölg, T., N. J. Cullen, D. R. Hardy, M. Winkler, and G. Kaser (2009), Quantifying climate change in the tropical midtroposphere over East Africa from glacier shrinkage on Kilimanjaro, *J. Clim.*, *22*, 4162–4181, doi:10.1175/2009JCLI2954.1.
- Mölg, T., F. Maussion, and D. Scherer (2014), Mid-latitude westerlies as a driver of glacier variability in monsoonal High Asia, *Nat. Clim. Change*, *4*, 68–73, doi:10.1038/nclimate2055.
- National Meteorological Information Center (2005), Documentation of China's upper standard layer monthly dataset V2.0, NMIC-CMA, Beijing, China.
- Ohmura, A., P. Kasser, and M. Funk (1992), Climate at the equilibrium line of glaciers, *J. Glaciol.*, *38*, 397–411.
- Pepin, N. C., and J. D. Lundquist (2008), Temperature trends at high elevations: Patterns across the globe, *Geophys. Res. Lett.*, *35*, L14701, doi:10.1029/2008GL034026.
- Pepin, N. C., and D. J. Seidel (2005), A global comparison of surface and free-air temperatures at high elevations, *J. Geophys. Res.*, *110*, D03104, doi:10.1029/2004JD005047.
- Piao, S., et al. (2010), The impacts of climate change on water resources and agriculture in China, *Nature*, *467*, 43–51, doi:10.1038/nature09364.
- Pu, J., T. Yao, M. Yang, L. Tian, N. Wang, Y. Ageta, and K. Fujita (2008), Rapid decrease of mass balance observed in the Xiao (Lesser) Dongkemadi Glacier, in the central Tibetan Plateau, *Hydrol. Process.*, *22*, 2953–2958, doi:10.1002/hyp.6865.
- Qin, J., K. Yang, S. Liang, and X. Guo (2009), The altitudinal dependence of recent rapid warming over the Tibetan Plateau, *Clim. Change*, *97*, 321–327, doi:10.1007/s10584-009-9733-9.
- Rabatel, A., et al. (2013), Current state of glaciers in the tropical Andes: A multi-century perspective on glacier evolution and climate change, *Cryosphere*, *7*, 81–102, doi:10.5194/tc-7-81-2013.
- Schneider, U., A. Becker, P. Finger, A. Meyer-Christoffer, B. Rudolf, and M. Ziese (2011), GPCC Full Data Reanalysis Version 6.0 at 0.5°: Monthly land-surface precipitation from rain-gauges built on GTS-based and historic data, doi:10.5676/DWD_GPCC/FD_M_V6_050.
- Schneider, U., A. Becker, P. Finger, A. Meyer-Christoffer, M. Ziese, and B. Rudolf (2014), GPCC's new land surface precipitation climatology based on quality-controlled in situ data and its role in quantifying the global water cycle, *Theor. Appl. Climatol.*, *115*, 15–40, doi:10.1007/s00704-013-0860-x.
- Sen, P. K. (1968), Estimates of the regression coefficient based on Kendall's tau, *J. Am. Stat. Assoc.*, *63*, 1379–1389, doi:10.1080/01621459.1968.10480934.
- Shi, Y. (2008), *Concise Glacier Inventory of China*, Shanghai Popular Science Press, Shanghai, China.
- Simmons, A. J., P. D. Jones, V. da Costa Bechtold, A. C. M. Beljaars, P. W. Källberg, S. Saarinen, S. M. Uppala, P. Viterbo, and N. Wedi (2004), Comparison of trends and low-frequency variability in CRU, ERA-40, and NCEP/NCAR analyses of surface air temperature, *J. Geophys. Res.*, *109*, D24115, doi:10.1029/2004JD005306.
- Thurai, M., E. Deguchi, T. Iguchi, and K. Okamoto (2003), Freezing height distribution in the tropics, *Int. J. Satell. Commun. N.*, *21*, 533–545, doi:10.1002/sat.768.
- Vergara, W., A. Deeb, A. Valencia, R. S. Bradley, B. Francou, A. Zarzar, A. Grunwaldt, and S. Haeussling (2007), The economic impacts of rapid glacier retreat in the Andes, *Eos Trans. AGU*, *88*, 261–264, doi:10.1029/2007EO250001.
- Vuille, M., B. Francou, P. Wagnon, I. Juen, G. Kaser, B. G. Mark, and R. S. Bradley (2008), Climate change and tropical Andean glaciers: Past, present and future, *Earth Sci. Rev.*, *89*, 79–96, doi:10.1016/j.earscirev.2008.04.002.
- Wang, N., J. He, J. Pu, X. Jiang, and Z. Jing (2010), Variations in equilibrium line altitude of the Qiyi Glacier, Qilian Mountains, over the past 50 years, *Chinese Sci. Bull.*, *55*, 3810–3817, doi:10.1007/s11434-010-4167-3.
- Wang, S., M. Zhang, Z. Li, F. Wang, H. Li, Y. Li, and X. Huang (2011), Glacier area variation and climate change in the Chinese Tianshan Mountains since 1960, *J. Geogr. Sci.*, *21*, 263–273, doi:10.1007/s11442-011-0843-8.
- Wang, X. L. (2008), Accounting for autocorrelation in detecting mean shifts in climate data series using the penalized maximal t or F test, *J. Appl. Meteorol. Climatol.*, *47*, 2423–2444, doi:10.1175/2008JAMC1741.1.
- WGMS (World Glacier Monitoring Service) (2005), *Fluctuations of Glaciers 1995–2000*, vol. VIII, IUGG (CCS) – UNEP – UNESCO, Zurich, Switzerland.

- WGMS (World Glacier Monitoring Service) (2008), *Fluctuations of Glaciers 2000–2005*, vol. IX, ICSU (FAGS) – IUGG (IACS) – UNEP – UNESCO – WMO, Zurich, Switzerland.
- WGMS (World Glacier Monitoring Service) (2012), *Fluctuations of Glaciers 2005–2010*, vol. X, ICSU (WDS) – IUGG (IACS) – UNEP – UNESCO – WMO, Zurich, Switzerland.
- WGMS and NSIDC (1989, updated 2012), World Glacier Inventory, World Glacier Monitoring Service, Zurich, Switzerland, and the National Snow and Ice Data Center, Boulder, Colo., USA, doi:10.7265/NS/NSIDC-WGI-2012-02.
- Xu, W., Q. Li, X. L. Wang, S. Yang, L. Cao, and Y. Feng (2013), Homogenization of Chinese daily surface air temperatures and analysis of trends in the extreme temperature indices, *J. Geophys. Res. Atmos.*, *118*, 9708–9720, doi:10.1002/jgrd.50791.
- Yao, T., et al. (2012), Different glacier status with atmospheric circulations in Tibetan Plateau and surroundings, *Nat. Clim. Change*, *2*, 663–667, doi:10.1038/nclimate1580.
- Ye, B., D. Yang, K. Jiao, T. Han, Z. Jin, H. Yang, and Z. Li (2005), The Urumqi River source Glacier No. 1, Tianshan, China: Changes over the past 45 years, *Geophys. Res. Lett.*, *32*, L21504, doi:10.1029/2005GL024178.
- You, Q., K. Fraedrich, G. Ren, N. Pepin, and S. Kang (2013), Variability of temperature in the Tibetan Plateau based on homogenized surface stations and reanalysis data, *Int. J. Climatol.*, *33*, 1337–1347, doi:10.1002/joc.3512.
- Yue, S., and C. Y. Wang (2002), Applicability of prewhitening to eliminate the influence of serial correlation on the Mann-Kendall test, *Water Resour. Res.*, *38*(6), 1068, doi:10.1029/2001WR000861.
- Yue, S., P. Pilon, B. Phinney, and G. Cavadas (2002), The influence of autocorrelation on the ability to detect trend in hydrological series, *Hydrol. Process.*, *16*, 1807–1829, doi:10.1002/hyp.1095.
- Zhang, G., S. Sun, Y. Ma, and L. Zhao (2010), The response of annual runoff to the height change of the summertime 0°C level over Xinjiang, *J. Geogr. Sci.*, *20*, 833–847, doi:10.1007/s11442-010-0814-5.
- Zhang, J., X. He, B. Ye, and K. Wu (2013), Recent variation of mass balance of the Xiao Dongkemadi Glacier in the Tanggula Range and its influencing factors, *J. Glaciol. Geocryol.*, *35*, 263–271, doi:10.7522/j.issn.1000-0240.2013.0032.
- Zhang, M., S. Wang, Z. Li, and F. Wang (2012), Glacier area shrinkage in China and its climatic background during the past half century, *J. Geogr. Sci.*, *22*, 15–28, doi:10.1007/s11442-012-0908-3.
- Zhang, Y., and Y. Guo (2011), Variability of atmospheric freezing-level height and its impact on the cryosphere in China, *Ann. Glaciol.*, *52*, 81–88, doi:10.3189/172756411797252095.